DOI 10.1007/s11595-016-1521-6

Microstructures and Mechanical, Electrical, High-temperature Properties of Cu/Ti_2AlC FGM Fabricated by Hot-pressing

CHEN Yanlin[1,2], LI Jin[3], LIU Hao[3], LI Zongyu[3], ZENG Chengwen[3]

(1. Hubei Provincial Key Laboratory of Green Materials for Light Industry, Hubei University of Technology, Wuhan 430068, China; 2. Collaborative Innovation Center of Green Light-weight Materials and Processing, Hubei University of Technology, Wuhan 430068, China; 3. School of Materials Science and Engineering, Hubei University of Technology, Wuhan 430068, China)

Abstract: The microstructure and the electrical, thermal, friction, and mechanical properties of Cu/Ti_2AlC fabricated by hot-pressing at 900 ℃ for 1 h were investigated in the present work. Microstructural observations have shown that the plate-like Ti_2AlC grains distribute irregularly in the network of Cu grains, and well-structured, crack-free bonds between the layers. With the increase in the content of Ti_2AlC from layer A to layer D, the electrical resistivity increases from $1.381\times10^{-7}\,\Omega\cdot m$ to $1.918\times10^{-7}\,\Omega\cdot m$, the hardness increases from about 980.27 MPa to about 2196.01 MPa, and the friction coefficient from above 0.20 reduces to about 0.15. Oxidation rate increases with the increases of temperature. Exfoliation was obviously observed on the surface of oxidation layer A. The surface of layer D was still intact and the spalling and other defects were not found. The mass decreases in the acid solution, and increases in the alkaline solution. The largest corrosion rate is found in 6.5% HNO_3 or 4% NaOH solution.

Key words: functional gradient material; Cu/Ti_2AlC; preparation; performance

1 Introduction

Cu possesses high heat conductance, good electric conductivity and machinability, and is widely used in cable transformer, switch, plug components, pantograph slide and resistance welding electrode, *etc*[1]. However, its lower strength, hardness, abrasion resistance and oxidability at high temperature were often the main reason for limiting their applications. The materials not only need high electrical conductivity, thermal conductivity and low temperature ductility, but also high strength, oxidation resistance and good wear resistance[2].The introduction of the enhancement phase to improve the strength and hardness of the materials at the same time will significantly reduce the electrical conductivity and thermal conductivity properties of the materials. It is difficult to balance their properties, such as electric conduction, strength and hardness. Otherwise, it has self-lubrication owing to its layered structure[3,4]. Ti_2AlC, as a new layered ternary ceramic, has attracted many attentions of researchers owing to its unique properties, which combine unusual properties of both ceramics and metals. Like ceramics, it exhibits high rigidity, rupture tenacity, excellent corrosion resistance and high temperature oxidation. Like metals, it combines good thermal conductivity (46×10^{-6} W/K) and electrical conductivity ($3.7\times10^{-7}\,\Omega\cdot m$), is relatively soft and can be easily machined with traditional drill.

With the development of science and technology, the demand on their property has also been on the rise. For Cu/Ti_2AlC composite material, it is difficult to completely meet operating requirement due to lower hardness and strength with high Cu phase. When the content of Ti_2AlC phase is higher, the material toughness is low, so it is vulnerable to brittle fracture. Hence considerable research has been done, and Cu base functionally graded materials were mainly Cu-Mo, Cu-W[5-8], Cu-Ni[9], and Cu-Al_2O_3[10] series. Functionally graded materials (FGM), as a kind of new type heterogeneous materials, with both composition and

(Received: Jan. 14, 2016; Accepted: Mar. 20, 2016)

CHEN Yanlin(陈艳林): Assoc. Prof.; E-mail: chenyl70@126.com

The Open Foundation of Hubei Provincial Key Laboratory of Green Material for Light Industry(No. (2013)2-general project-9), the Key Project of Education Department of Hubei(No. D20131406), and the National Natural Science Foundation of China(No. 51302073)

performance gradually changing along the thickness direction[11], can deal with the issues. Cu/Ti_2AlC FGMs have high hardness, strength and toughness. When great impact is loaded, the side of Cu rich withstands large deformation because of its high toughness of materials, and another side of Ti_2AlC rich bores greater force and reduces deformation due to its high strength and hardness[12-15]. Therefore, its application scope and life are greatly increased. When both sides of Cu/Ti_2AlC are at different temperatures, thermal expansion of the side at higher temperature is higher than that of the other, which results in high thermal stress because of thermal expansion differences. However, for Cu/Ti_2AlC FGMs, the composition and performance of both sides are different. Thermal expansion coefficient of the side at high temperature is lower than that of the other. Thermal stress of the material is small since thermal expansion of the whole distributes evenly.

In this paper, Cu base functionally graded materials were prepared by introducing Ti_2AlC phase as the reinforced phase. Cu/Ti_2AlC FGM was produced by hot-pressing in a vacuum. The advantage of this material is that it has not only high mechanical strength and oxidation resistance, but also good friction properties, high heat and electrical conductivity.

2 Experimental

Raw materials for the experiment were commercial powders including Al powder (99.7%), Ti powder (99.5%), TiC powder (99.5%), and Cu powder (99.6%). The powders of Ti_2AlC were obtained by means of crush and mill from sintered compact using Ti, Al and TiC powders by hot-pressing at 900 ℃ for 1 h. In order to study the performance of layers and bulk, Cu/Ti_2AlC composite materials and Cu/Ti_2AlC FGMs of 4 layers were fabricated by hot-press sintering process at 900 ℃ for 1 h under 30 MPa in a vacuum. The first layer was for Cu-5%Ti_2AlC (Layer A), the second for Cu-20%Ti_2AlC (Layer B), the third layer for Cu-40%Ti_2AlC (Layer C), the fourth layer for Cu-60%Ti_2AlC (Layer D), and the mass of each layer was 1 g. The sample with diameter of Φ15mm was obtained. The density was determined by the Archimedes method. The microstructure and fracture surface were observed on an optical microscope (XJZ-6, Jiangnan, China) and a scanning electron microscope (SEM, JSM6390, JEOL, Japan) equipped with energy-dispersive spectroscopy (EDS).The phase compositions were analysed by XRD (D/MAX-RB, RIGAKU, Japan). The Vickers hardness was measured with a hardness analyzer (HVS-1000, Huayinu, China). The electrical resistivity was measured by a four-point probe tester (SZT-2A, Shuangx, China). The friction coefficient was tested by a friction and wear tester (CSM/60N, CSM, Switzerland).

3 Results and discussion

3.1 Relative density

As listed in Table 1, all the actual density, theoretical density and relative density of graded layers decrease with increasing in the volume fraction of Ti_2AlC. The relative densities decrease from 99.20% for Cu-5%Ti_2AlC to 94.16% for Cu-60%Ti_2AlC, and the relative density of the whole was 96.93%. The density of Ti_2AlC (4.11 g/cm^3) is much less than that of Cu (8.96 g/cm^3). The increase in the percentage of Ti_2AlC makes the actual density and theoretical density trend to the density of Ti_2AlC. So the actual density and theoretical density decrease with the increase in the percentage of Ti_2AlC. The lower the melting point, the higher diffusivity is due to the weaker atomic bonding energy. Sintering temperature is close to that of Cu (1083 ℃) and far from that of Ti_2AlC, so the densification of Cu/Ti_2AlC is mainly dependent on plastic flow and the diffusion of Cu. With the increase of Ti_2AlC, plastic phase Cu decreases and the diffusion process slows, so the relative density decreases with increasing porosity.

According to the theory of plastic flow,

$$\ln\frac{1}{(1-\rho_E)}=\frac{\sqrt{2}\gamma n^{1/3}}{\tau_c}\left(\frac{1-\rho_E}{\rho_E}\right)^{1/3}\cdot\left(\frac{3}{4\pi}\right)^{1/3}+\frac{P}{\sqrt{2}\tau_c} \quad (1)$$

When hot-pressing temperature is constant, increasing hot-pressing pressure can improve the density. When the pressure stays the same temperature density is also improved.

3.2 Phase composition and microstructure

XRD patterns of the samples with different layer contents are shown in Fig.1. The samples are mainly composed of Cu, Ti_2AlC and TiC, and the peaks of Ti_2AlC and TiC enhance with the increase in the content of Ti_2AlC. In the sintering process of Cu/Ti_2AlC FGM, the bonding strength of Ti-Al was weak. Al atoms are easy to break loose from atomic force bond and dissolve to Cu crystal structure in the heat. Thus Cu-Al alloy and TiC formed. Fracture surfaces of graded layers are shown in Fig.2. Structure morphologies of Cu and Ti_2AlC are mostly network and lamellar

respectively by EDS. When the volume fractions of Ti_2AlC are 5% and 20%, Ti_2AlC particles irregularly distribute in the network structures. The fracture of sample has dimple pattern by localized necking with features of plastic fracture, and the grain size is mostly 3-6 μm. The amount of lamellar grrain increases with the decrease of network grain and dimples.

Table 1 Density and relative density with different layers and the whole

Sample	Actual density /(g/cm^3)	Theoretical density /(g/cm^3)	Relative density /%
A	8.66	8.73	99.20
B	7.89	8.03	98.26
C	6.78	7.10	95.50
D	5.80	6.16	94.16
Bulk	7.28	7.51	96.93

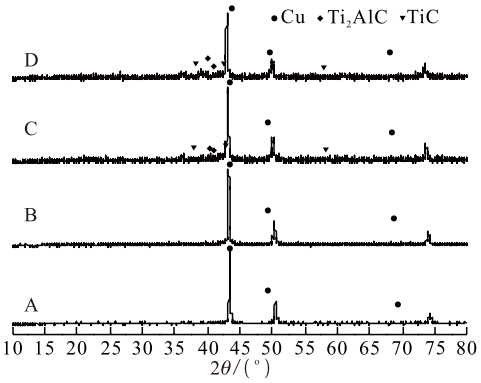

Fig.1 XRD patterns of D layer

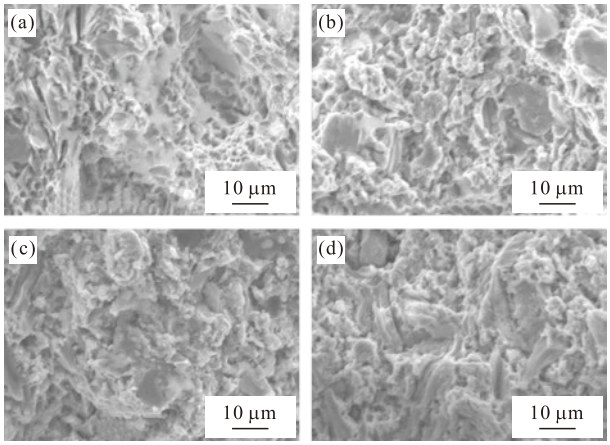

Fig.2 Fracture morphologies of different layers: (a)A layer; (b)B layer; (c)C layer; (d)D layer

3.3 Physical properties

As illustrated in Table 2, the resistivity of each layer increases with the increase in Ti_2AlC. The resistivity of the bulk is 1.583×10^{-7} Ω·m, below that of layer D (1.918×10^{-7} Ω·m) and above that of layer A (1.381×10^{-7} Ω·m). According to the following formula[4]:

$$\rho=\frac{\rho_0}{\left(1-\frac{1}{1+0.87\frac{1}{c}}\right)} \tag{2}$$

where, c is the volume fraction of Ti_2AlC at Cu-based composites. With increased content of Ti_2AlC, the continuity of Cu with higher electric conductivity is partly destroyed, and the resistivity of bulk is greater than that of layer C and D.

The results of Vickers hardness measured across all layers from A to D are shown in Fig.3. From layer A to layer D, the hardness increases markedly, from about 980.27 MPa to about 2196.01 MPa. The hardness of Ti_2AlC as ceramic phase is far higher than that of Cu metal. Hardness of composites layers has been strengthened by adding Ti_2AlC, and gradual transits from a layer to another with diffusion at interlayer.

Table 2 Resistivity of different layers and the bulk

Sample	A	B	C	D	Bulk
Resistivity/(10^{-7} Ω · m)	1.381	1.443	1.758	1.918	1.583

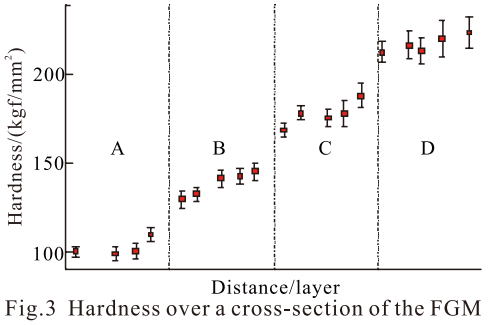

Fig.3 Hardness over a cross-section of the FGM

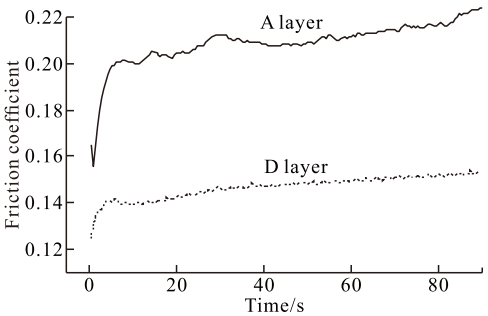

Fig.4 Friction coefficient of surface layer with time

The relationship between friction coefficient of surface layer and time of friction is shown in Fig.4. Friction coefficient decreases from above 0.2 to below 1.5 with the increase of Ti_2AlC. Friction coefficient reduces and achieves a minimum because of the self-lubrication of Ti_2AlC. It benefits sliding during friction wear and for stronger rigidity the contacting area of

friction pair is decreased. So both sides of FGM have different friction and wear performances to adopt different usage environments.

3.4 Antioxidant, anticorrosion and thermal shock properties

The changes of weight with time at different temperatures in oxidation experiment are shown in Fig.5. With the increase of time, the mass increases gradually and the trend slows down. The basis of the reaction is as follows[16]:

$$2Cu+O_2 \rightarrow 2CuO \quad (1)$$

$$4Ti_2AlC+5O_2 \rightarrow 4TiC+2Al_2O_3+4TiO_2 \quad (2)$$

The additional weight comes from CuO, Al_2O_3 and TiO_2. As the temperature rises, the rate of oxidation reaction increases. The oxidation rate at 500 ℃ is slow, and the additional weight is only 2.69×10^{-4} g/cm^2 even after oxidization for 20 hours. The weight increments are much more at 600 ℃ and 700 ℃. Exfoliation is obviously observed on the oxidation surface of layer A, as shown in Figs.6(a)-(c). The surface of layer D is still intact and the spalling and other defects are not found after oxidation for a long time, as shown in Figs.6(d)-6(f). The subscripts ox and m represent oxidation and substrate, respectively. Generally, peeling is caused by the thermal stress due to the mismatch in the thermal expansion coefficients of different materials. Thermal expansion coefficient of Ti_2AlC is 8.4×10^{-6} K, close to that of Al_2O_3 (8.8×10^{-6} K) and TiO_2 (9.1×10^{-6} K) [17]. Thermal expansion coefficient of Cu is 17.5×10^{-6} K, while that of CuO is below 10×10^{-6} K. For this reason, the peeling easily occurs on the surface of layer A, which contains more CuO, while much less peeling occurs at layer D. Oxidation reaction is restrained by oxidation products Al_2O_3 and TiO_2. The weight increment of oxidation mainly comes from layer A, on which new surface is generated continually due to the exfoliation of the old surface. But oxidation rate slows down because contacting area with oxygen reduces for accumulation of exfoliation over time.

The dependence of the square of the weight increment with time for sample oxidization at different temperatures is shown in Fig.7. The curves are nearly linear, and their slopes increase with increasing temperature. Therefore, the process of oxidation follows the parabolic law. The relationship between weight increment and time can be calculated by the equation:

$$(\Delta W/S)^2=k_p t \quad (3)$$

where, $\Delta W/S$ is the weight increment of sample, and k_p is the parabolic rate constant in oxidation, and t is the oxidation time. The values of k_p at different temperatures are shown in Table 3, from which it can be found that the parabolic rate constant at 600 ℃ and 700 ℃ is one order of magnitude higher than that at 500 ℃. Incompletely peeling on copper-rich surface prevents the oxidizing reaction to a certain extent.

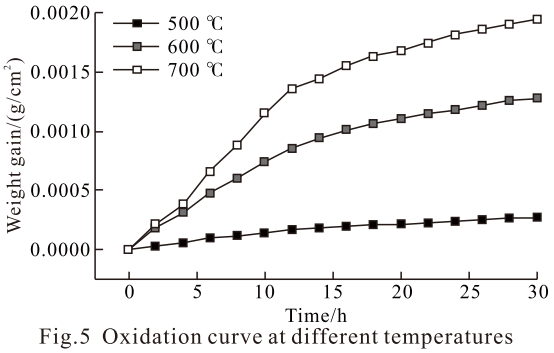

Fig.5 Oxidation curve at different temperatures

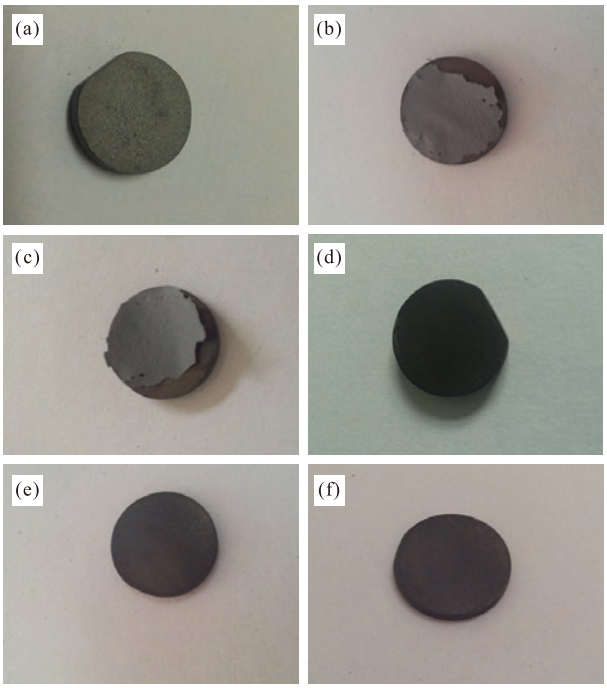

Fig.6 Appearance of different layers after oxidation for 6 h at different temperatures: (a) 500 ℃, layer A; (b) 600 ℃, layer A; (c) 700 ℃, layer A; (d) 500 ℃, layer D; (e) 600 ℃, layer D; (f) 700 ℃, layer D

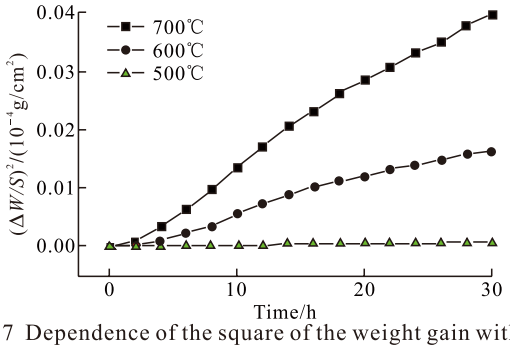

Fig.7 Dependence of the square of the weight gain with time for sample oxidization at different temperature

Table 3 Parabolic rate constants at different temperatures

Temperature/℃	Parabolic rate constant $k_p/(g^2 \cdot cm^{-4} \cdot s^{-1})$
500	$1.805\,6 \times 10^{-12}$
600	$1.185\,2 \times 10^{-12}$
700	$0.248\,9 \times 10^{-12}$

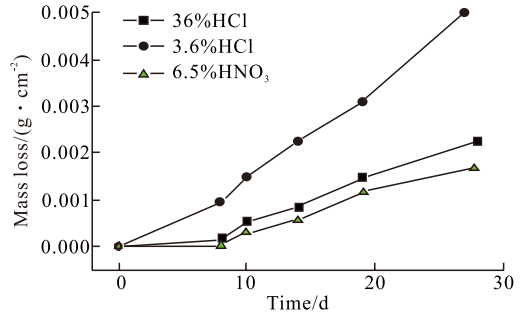

Fig.8 Mass loss curves for specimens immersed in acid solution

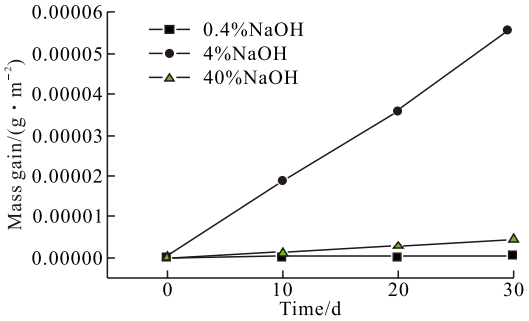

Fig.9 Mass gain curves for specimens immersed in alkali solution

Weight loss curves for specimens immersed in acid solution are shown in Fig.8. Weight loss rate of sample in HNO_3 was greater than that in HCl solution, and weight loss rate of sample in 36% HCl was greater than that in 3.6% HCl. Copper is prone to react with HNO_3 but not to react with HCl. So the weight loss of Cu and Ti_2AlC in HCl solution is perhaps caused by electrochemical corrosion. Weight increment curves for specimens immersed in alkali solution are shown in Fig.9. According to the research by Wang[18], the mass of Ti_2AlC bulk in NaOH will lower with time. The weight increment comes from Cu, which reacts with NaOH and CO_2 to form another species. The most weight increment occurs in 4% NaOH solution, then is 40% NaOH, and the least is 0.4% NaOH. In 0.4% NaOH, corrosion almost did not occur due to the small concentration of alkali. In 40% NaOH, passivation prevents the going on of the reaction.

4 Conclusions

Cu/Ti_2AlC FGM was fabricated by hot-press sintering under the pressure of 30 MPa at 900 ℃ for 1 h. The relative densities of the samples are higher than 96%. The fracture types change from a plastic fracture to a brittle fracture from layer A to D, and micro-structural observations have shown the good bonds between the layers.

Resistivity, hardness and friction coefficient were studied. From layer A to D, the surface resistivity gradually increases from 1.381×10^{-7} Ω·m to 1.918×10^{-7} Ω·m. Hardness increases from 980.27 MPa for layer A to the maximum of 2196.01 MPa for layer D, and friction coefficient reduces from above 0.20 to about 0.15. Oxidation resistance of samples obviously enhances with the increase in the content of Ti_2AlC. Thermal shock resistance is good owing to the mitigation effect of thermal stresses. The mass decreases in the acid solution and increases in the alkaline solution.

References

[1] Ma B, Li J, Peng Z, *et al*. Structural Morphologies of Cu-Sn-Bi Immiscible Alloys with Varied Compositions[J]. *Journal of Alloys and Compounds*, 2012, 535: 95-101
[2] Yan M, Zeng CW, Li ZY, *et al*. Physical, Antioxidant and Thermal Shock Properties of Cu/Ti_2AlC Conductive Composites[J]. *Journal of Wuhan University of Technology Mater. Sci. Ed.*, 2013, 28(3): 413-415
[3] Amini S, Ni C. Processing, Microstructural Characterization and Mechanical Properties of a Ti_2AlC/Nanocrystalline Mg-matrix Composite[J]. *Composites Science and Technology*, 2009, 69: 414-420
[4] Dong S, Shi Y, Lei Y. Effects of TiB_2 Content on Properties of TiB_2/Cu Composite[J]. *Hot Working Technology*, 2002, 3: 347-349
[5] Ahangarkani M, Borgi S. The Effect of Additive and Sintering Mechanism on the Microstructural Characteristics of W-40Cu Composites[J]. *International Journal of Refractory Metals and Hard Materials*, 2012, 32: 39-44
[6] Roosta M, Baharvandi H. The Comparison of W/Cu and W/ZrC Composites Fabricated Through Hot-press[J]. *Journal of Refractory Metals and Hard Materials*, 2010, 28: 587-592
[7] Shen W, Li Q, Chang K. Manufacturing and Testing W/Cu Functionally Graded Material Mock-ups for Plasma Facing Components[J]. *Journal of Nuclear Materials*, 2007, 367: 1 449-1 452
[8] Zhou ZJ, Du J, Song SX. Microstructural Characterization of W/Cu Functionally Graded Materials Produced by a One-step Resistance Sintering Method[J]. *Journal of Alloys and Compounds*, 2007, 428: 146-150
[9] Rubio WM, Paulino HG, Silva ECN. Analysis, Manufacture and Characterization of Ni/Cu Functionally Graded Structures[J]. *Materials and Design*, 2012, 41: 255-265
[10] Huang AN, Kuo HP. A Study on the Transition between Neighbouring Drum Segregated Bands and Its Application to Functionally Graded Material Production[J]. *Powder Technology*, 2011, 212: 348-353
[11] Okayasu M, Sato R, Takasu S. Effects of Anisotropic Microstructure of Continuous Cast Al-Cu Eutectic Alloys on Their Fatigue and Tensile Properties[J]. *International Journal of Fatigue*, 2012, 42: 45-56
[12] Su B, Yan HG, Chen G, *et al*. Study on the Preparation of the SiCp/ Al-20Si-3Cu Functionally Graded Material Using Spray Deposition[J]. *Materials Science and Engineering A*, 2010, 527: 6 660-6 665
[13] Mazare L, Miranda G, Soares D, *et al*. On the Ability of Producing Copper-silver Functionally Graded Alloys by Using an Incremental Melting and Solidification Process[J]. *Journal of Materials Processing Technology*, 2009, 209: 5 702-5 710
[14] Sofiyev AH, Kuruoglu N, Turkmen M. Buckling of FGM Hybrid Truncated Conical Shells Subjected to Hydrostatic Pressure[J]. *Thin-Walled Structures*, 2009, 47: 61-72
[15] Bai Y, He X, Zhu C. Microstructures, Electrical, Thermal and Mechanical Properties of Bulk Ti_2AlC Synthesized by Self-Propagating High-Temperature Combustion[J]. *The American Ceramic Society*, 2012, 95: 358-364
[16] Chen Y. *Thermodynamics, Synthesis, Oxidation properties of Ti_2AlC and Cr_2AlC Ceramics*[D]. Beijing: General Research Institute of Nonferrous Metals, 2012
[17] Liu G, Ma L, Liu J. *Chemical Property Data Manual* [M]. Beijing: Chemical Industry Press of China, 2002: 256-257
[18] Wang JP, Mei BC, Zhou WB, *et al*. Corrosion Behavior of Layered Ternary Carbide Ti_2AlC in Acidic Solution[J]. *Journal of Inorganic Materials*, 2009, 24(2): 402-406